Intracellular degradation of microspheres based on cross-linked dextran hydrogels or amphiphilic block copolymers: A comparative Raman microscopy study

Henk-Jan van Manen[1]
Aart A van Apeldoorn[2]
Ruud Verrijk[3]
Clemens A van Blitterswijk[2]
Cees Otto[1]

[1]Biophysical Engineering Group, Institute for Biomedical Technology (BMTI), and MESA+ Institute for Nanotechnology, University of Twente, The Netherlands; [2]Polymer Chemistry and Biomaterials Group, Institute for Biomedical Technology (BMTI), University of Twente, The Netherlands; [3]OctoPlus, Zernikedreef 12, The Netherlands

Correspondence: Henk-Jan van Manen
Biophysical Engineering Group, Institute for Biomedical Technology (BMTI), and MESA+ Institute for Nanotechnology, University of Twente, PO Box 217, 7500 AE Enschede, The Netherlands
Tel +31 53 489 4612
Fax +31 53 489 1105
Email h.w.j.vanmanen@tnw.utwente.nl

Abstract: Micro- and nanospheres composed of biodegradable polymers show promise as versatile devices for the controlled delivery of biopharmaceuticals. Whereas important properties such as drug release profiles, biocompatibility, and (bio)degradability have been determined for many types of biodegradable particles, information about particle degradation inside phagocytic cells is usually lacking. Here, we report the use of confocal Raman microscopy to obtain chemical information about cross-linked dextran hydrogel microspheres and amphiphilic poly(ethylene glycol)-terephthalate/poly(butylene terephthalate) (PEGT/PBT) microspheres inside RAW 264.7 macrophage phagosomes. Using quantitative Raman microspectroscopy, we show that the dextran concentration inside phagocytosed dextran microspheres decreases with cell incubation time. In contrast to dextran microspheres, we did not observe PEGT/PBT microsphere degradation after 1 week of internalization by macrophages, confirming previous studies showing that dextran microsphere degradation proceeds faster than PEGT/PBT degradation. Raman microscopy further showed the conversion of macrophages to lipid-laden foam cells upon prolonged incubation with both types of microspheres, suggesting that a cellular inflammatory response is induced by these biomaterials in cell culture. Our results exemplify the power of Raman microscopy to characterize microsphere degradation in cells and offer exciting prospects for this technique as a noninvasive, label-free optical tool in biomaterials histology and tissue engineering.

Keywords: biodegradation, microspheres, Raman microscopy, phagocytosis, drug delivery

Introduction

Biopharmaceuticals, defined as "pharmaceutical products consisting of (glyco)proteins and nucleic acids" (Schellekens 2002), constitute an increasingly important class of therapeutic molecules used in medicine today. The growth of this category of medicines, which is faster than the introduction of new low-molecular-weight medicinal compounds, is fuelled to a large extent by current fast-paced developments in "-omics" disciplines such as genomics/transcriptomics, proteomics, and metabolomics (Nikolsky et al 2005). The application of systems biology (Butcher et al 2004) or molecular profiling (Stoughton and Friend 2005) strategies, in which various "-omics" data sets are integrated (Joyce and Palsson 2006), is anticipated to further boost drug discovery.

As therapeutic agents, biopharmaceutical macromolecules must be considered separately from their low-molecular-weight counterparts because of their very different properties (Crommelin et al 2003a). Characteristics such as a high hydrophilicity, a large size, a complicated three-dimensional structure, and a low stability render biopharmaceuticals i) sensitive towards (enzymatic) degradation, ii) poorly permeable

across biological membranes, and iii) therefore difficult to deliver to their targeted site by conventional routes such as oral, nasal, and transdermal delivery. The alternative, parenteral administration of proteins by subcutaneous or intramuscular injection may suffer from a high injection frequency due to the limited half-lives of the proteins and also from a high initial, potentially toxic concentration of the injected therapeutics. To produce the desired pharmacokinetic profile and to reduce the injection frequency and improve patient compliance, new micro- and nanoscale drug delivery systems (DDS) for the targeted, controlled release of macromolecules are continuously being developed (Crommelin et al 2003b).

Whereas most commercial DDS for parenteral delivery of therapeutics are based on nanosized liposomes (Allen and Cullis 2004), biodegradable polymeric micro- and nanoparticles are also under active investigation as versatile drug delivery vehicles (Cleland et al 2001; Edlund and Albertsson 2002; Sinha and Trehan 2003). In particular, nano- and microspheres based on FDA-approved polyesters such as poly(lactic(-*co-glycolic*) acid) (PL(G)A) have been put forward as suitable protein delivery systems because of their favorable biodegradation and biocompatibility characteristics (Anderson and Shive 1997; Panyam and Labhasetwar 2003). However, problems with protein unfolding, aggregation, and degradation, combined with the limited possibility to control protein release rates, may compromise the suitability of PLGA as polymeric vehicle for high-molecular-weight protein drugs (Van de Weert et al 2000). Therefore, alternative biocompatible polymers that offer a milder environment are being developed and studied for their protein encapsulation and release characteristics. DDS based on amphiphilic block copolymers (Kumar et al 2001) or cross-linked hydrogels (Peppas et al 2000; Gupta et al 2002; Hoffman 2002) have generated much interest because of their favorable qualities in this regard. For example, a series of poly(ether-ester) multiblock copolymers based on hydrophilic poly(ethylene glycol)-terephthalate (PEGT) and hydrophobic poly(butylene terephthalate) (PBT) segments (Figure 1b) has been introduced as matrix for controlled release applications (Bezemer et al 1999, 2000a, 2000b, 2000c).

The biocompatibility, biodegradability, and quantitative release of fully active proteins has been demonstrated for these PEGT/PBT copolymers in both in vitro and in vivo studies (Bezemer et al 2000a; Van Dijkhuizen-Radersma et al 2002; Deschamps et al 2004). In addition to these desirable DDS properties, hydrogels display the additional advantage of providing a very protein-friendly environment because their three-dimensional, cross-linked hydrophilic network imposes a high aqueous content with a physiological pH. In recent years, we have developed biodegradable hydrogel microspheres based on cross-linked dextran polymers for drug delivery purposes. Starting from low-molecular-weight dextran derivatized with 2-hydroxyethylmethacrylate (HEMA) moieties (ie, dex-HEMA, Figure 1a) (Van Dijk-Wolthuis et al 1997b), chemical cross-linking of the dextran polymer chains by radical polymerization of the methacrylate units in a water-in-water microdroplet emulsion provides hydrogel microspheres with diameters ranging from 2 to 20 μm (Stenekes et al 1998). Enrichment of the dextran phase with pharmaceutical proteins prior to the cross-linking step results in microspheres with high protein encapsulation efficiencies (>90%). The release rate of proteins from the dextran microspheres can be tailored by varying the cross-link density (represented by the degree of substitution [DS], ie, the number of HEMA side chains per 100 glucose units) and the initial water content of the hydrogel (Franssen et al 1999). Release kinetics also depend on the hydrolysis rate of the hydrolytically sensitive carbonate esters in the cross-links, which in turn depends on the pH (Franssen et al 1999). Controlled in vitro release of IgG (Franssen et al 1999) and liposomes (Stenekes et al 2001) from cross-linked dextran microspheres have been successfully demonstrated. The therapeutic performance of microspheres loaded with interleukin-2 (De Groot et al 2002) has been investigated in mouse
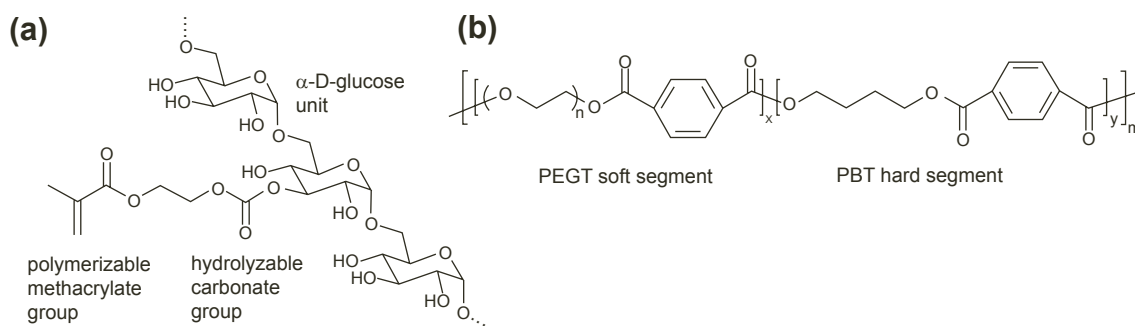

Figure 1 Chemical structures of 2-hydroxyethylmethacrylate-derivatized dextran (**a**) and amphiphilic PEGT/PBT segmented block copolymers (**b**).

models. It was found that when the drug is encapsulated by the microspheres, the injection frequency can be reduced without compromising the therapeutic efficacy.

Although it has been reported that cross-linked dextran microspheres are well tolerated after subcutaneous injection in rats (Cadée et al 2001), their intracellular degradation and drug release properties have not been addressed. Through phagocytosis, the internalization of particulate matter by specific cells, microspheres (~0.5–10 µm) loaded with therapeutics may be selectively targeted to professional phagocytes such as neutrophils, macrophages, and dendritic cells. Because these cells are critical in the innate and adaptive immune response, targeted delivery of drugs to them using degradable microspheres may allow one to modulate their immune response (Raychaudhuri and Rock 1998) in cases where this is desired, for example in autoimmune diseases (Feldmann and Steinman 2005). Moreover, macrophages and dendritic cells are professional antigen-presenting cells and thus represent targets for vaccine delivery (Banchereau and Steinman 1998). With such applications in mind, it is of great interest to study the biodegradation rate and release properties of polymeric microspheres inside phagocytes. Single-cell Raman micro(spectro)scopy (see eg, Uzunbajakava et al 2003; Van Manen et al 2005; Chan et al 2006; Krafft et al 2006; Notingher and Hench 2006), which enables detailed chemical information about intracellular constituents to be obtained in a label-free manner, is a noninvasive technique that is well-suited for such investigations. Using Raman microscopy, we have previously reported that extensive hydrolysis of ester bonds in PLGA microspheres occurs upon prolonged (1–2 weeks) internalization of these microspheres by macrophages (Van Apeldoorn et al 2004). Due to the above-mentioned, potential problems of using PLGA microspheres for the controlled release of proteins, it is of interest to study the degradation of other biodegradable microspheres inside phagocytes. Here, we present a Raman microscopy study of microspheres composed of cross-linked dextran hydrogels and amphiphilic PEGT/PBT block copolymers that have been internalized by murine RAW 264.7 macrophages for up to 3 weeks in in vitro cell culture systems. We show that, whereas PEGT/PBT microspheres do not show intracellular degradation by Raman microscopy after 1 week, the relative concentration of dextran in cross-linked dextran microspheres decreases to a large extent upon prolonged phagocytosis by macrophages. These results are consistent with previous studies of subcutaneously injected microspheres of these materials, which indicate that in vivo degradation of dextran hydrogel microspheres proceeds faster than PEGT/PBT microsphere degradation (Cadée et al 2001; Van Dijkhuizen-Radersma et al 2002). Furthermore, it is shown that both types of microspheres may induce inflammation in macrophages in which they reside for multiple days, as judged from the foam-cell appearance of microsphere-containing macrophages. This is not unexpected, since phagocytosis is known to elicit both innate immune responses, aimed at destruction of the internalized particulate matter, and inflammatory responses (Greenberg and Grinstein 2002). Finally, our results underscore the suitability of Raman microscopy for the noninvasive study of biomaterials degradation in cells and tissues. A particular advantage of Raman microscopy, which has hardly been exploited for this purpose, is that chemical information can be obtained from both the (degrading) biomaterial and its surrounding intra- or extracellular environment in the same experiment.

Materials and methods
Materials
Poly(ethylene glycol) (PEG) 10,000 g/mol and sodium peroxodisulfate were obtained from Merck (Darmstadt, Germany), *N,N,N′,N′*-tetramethylethylenediamine (TEMED) was obtained from Fluka (Buchs, Switzerland), and poly-L-lysine hydrobromide was obtained from Sigma-Aldrich (Zwijndrecht, The Netherlands). Hydroxyethylmethacrylate-derivatized dextrans (dex-HEMA) with a degree of substitution (DS), ie, the number of HEMA side chains per 100 glucose units, of 8 and 16 were synthesized according to a published procedure (Van Dijk-Wolthuis et al 1997b). CaF$_2$ slides for Raman microscopy were obtained from Spectroscopy Central Ltd (Warrington, UK) and coated with 0.01% poly-L-lysine as described (Van Manen et al 2004).

Preparation of dextran hydrogel DS 8 and DS 16 microspheres
Cross-linked dextran microspheres were prepared by a reported water-in-water emulsion procedure (Stenekes et al 1998). All solutions were prepared in 25 mM sodium phosphate buffer pH 7.0 (referred to as "buffer"). First, dex-HEMA (61 mg for both DS 8 and DS 16) and PEG (2.0 g) were dissolved in 0.55 ml and 3.0 ml buffer, respectively. Second, 3.32 g PEG solution + 1.07 g buffer (DS 8) or 3.25 g PEG solution + 1.14 g buffer (DS 16) were added to the dex-HEMA solutions in 15-ml tubes. By vortexing these mixtures for 1 min at maximum speed (Vortex Genie 2, model G560E, Scientific Industries, Inc., Bohemia, NY), water-in-water emulsions were obtained. Next, 100 µl of TEMED solution (20% v/v,

pH neutralized with 4 M hydrochloric acid) was added to each emulsion. After vortexing for 1 min at maximum speed, 180 µl of sodium peroxodisulfate solution (44 mg/ml) was added to each emulsion. The tubes were gently tumbled 3×, and polymerization was allowed to proceed for 1 h at room temperature without stirring. The cross-linked dextran microspheres were centrifuged for 20 min at 3500 rpm, and the resulting pellets (~120 mg of hydrogel per batch) were resuspended in buffer. Multiple washing and centrifugation cycles were applied to further purify the microspheres.

In vitro degradation of dextran microspheres

To hydrolyze the carbonate ester bonds in cross-linked dextran microspheres, suspensions of microspheres in 0.05 M NaOH were incubated overnight at 37 °C. Free dextran was removed from the poly(HEMA) microspheres by repeated washing and centrifugation cycles.

Preparation of PEGT/PBT microspheres

Microspheres of the 1000PEGT70PBT30 copolymer, in which the PEG molecular weight is 1000, the wt% of PEG terephthalate is 70, and the wt% of PBT is 30, were prepared by an oil-in-water emulsion method as described before (Van Dijkhuizen-Radersma et al 2002).

Cell culture

Murine RAW 264.7 macrophages (obtained from the European Collection of Cell Cultures) were maintained in RPMI-1640 medium supplemented with 10% (v/v) fetal calf serum, 2 mM glutamine, 100 U/ml penicillin, and 50 µg/ml streptomycin at 37 ºC in a 5% CO_2 atmosphere.

Phagocytosis of dextran hydrogel or PEGT/PBT microspheres

RAW 264.7 macrophages were adhered to poly-L-lysine-coated CaF_2 slides and grown overnight. Dextran hydrogel or PEGT/PBT microspheres, which had been serum-opsonized as described before (Van Manen et al 2004), were added to the slides and the samples were incubated for 3 h at 37 °C in culture medium (see above). After washing with PBS, incubation in culture medium was continued for varying periods of time (see the Results and Discussion section). Slides were washed with PBS and cells were subsequently fixed for 1 h in 2% paraformaldehyde in PBS at room temperature. During Raman microscopy experiments slides were kept in Petri dishes filled with PBS.

Confocal Raman microspectroscopy and imaging

Raman spectroscopy and imaging experiments were performed on a previously described laser-scanning confocal Raman microspectrometer (Uzunbajakava et al 2003) equipped with a Kr^+ laser (Innova 90-K; Coherent, Santa Clara, CA), a 63×/1.2 NA water-immersion objective (Plan Neofluar; Carl Zeiss, Jena, Germany), a 25 µm pinhole, a holographic grating-containing spectrograph (HR460; Jobin-Yvon, Paris, France), and a back-illuminated CCD detector (1100 PB/Visar; Princeton Instruments, Trenton, NJ). Imaging experiments were performed by raster-scanning the laser beam over a microsphere, a cell, or an intracellular region of interest and accumulating a full Raman spectrum at each pixel (typically 1 s/pixel at 100 mW 647.1 nm excitation power). Noise in the resulting 3D (spatial × spatial × spectral dimension) data matrix was reduced by singular value decomposition (Uzunbajakava et al 2003). Raman images were constructed by plotting the integrated intensity of the vibrational band of interest as a function of position. Hierarchical cluster analysis (HCA) was performed on Raman imaging data matrices to visualize regions in cells with high Raman spectral similarities. In the cluster analysis routine, principal component analysis scores were taken as input variables, squared Euclidean distances were used as distance measure, and Ward's algorithm was employed to partition Raman spectra into clusters. All data manipulations were performed in routines written in MATLAB 6.5 (The MathWorks, Inc., Natick, MA).

For each type of microsphere (dextran hydrogel DS8, DS16, and 1000PEGT70PBT30 microspheres) phagocytosed by RAW 264.7 macrophages, 6–10 Raman images on different cells were recorded for every incubation time (see Results and Discussion). The Raman images displayed in Figures 3, 5, 6, and 8 are representative examples from these image data sets.

Quantification of the relative dextran concentration in the center of microspheres using the Raman band of water as an internal intensity standard

From each Raman imaging data set, an average buffer spectrum was obtained by averaging 50 spectra taken from regions outside the microsphere or cell. Baselines were subtracted from the resulting buffer spectra, which were also truncated to the 1400–1800 cm^{-1} spectral region. For each Raman image, an integrated Raman intensity, I_{water}, was obtained by integrating the intensity of the Raman band of

water at 1640 cm^{-1}. Next, hierarchical cluster analysis was performed on the same Raman imaging data sets, and average spectra of clusters corresponding to the central region of microspheres (freshly prepared or incubated with RAW 264.7 macrophages for various periods) were subjected to baseline subtraction. Finally, the intensity of the 541-cm^{-1} Raman band of dextran in these baseline-corrected cluster spectra, I_{dex}, was divided by I_{water} from the same Raman image to provide the I_{dex}/I_{water} ratio.

Results and discussion
Raman microscopy of freshly prepared and chemically hydrolyzed dextran hydrogel microspheres

To characterize the molecular composition of cross-linked dex-HEMA hydrogel microspheres and to visualize the distribution of dextran inside these microspheres, Raman imaging experiments were performed on freshly prepared microspheres (see Materials and methods) that had adhered to glass cover slips. By raster-scanning the Raman excitation beam ($\lambda_{exc} = 647.1$ nm) over a region of interest and accumulating a full Raman spectrum (spectral range 0–2000 cm^{-1})

at each position, Raman images were constructed from the resulting 3D data sets (spatial × spatial × spectral dimension) by plotting the intensity of a Raman band of interest as a function of position. Representative Raman images, constructed from the strong 541-cm^{-1} vibrational band of dextran, of cross-linked dex-HEMA microspheres are shown in Figure 2a and 2b.

The average Raman spectrum from the microsphere displayed in Figure 2a is shown in Figure 2c. As expected, the most intense Raman signals from the microspheres can be assigned to dextran (Zhbankov et al 2000). The overlapping weak broad bands centered at ~1712 cm^{-1} and ~1750 cm^{-1} are assigned to the methacrylate and carbonate ester C=O stretching vibrations of dex-HEMA, respectively. Values of 1718 cm^{-1} and 1752 cm^{-1}, obtained by FTIR spectroscopy on dex-HEMA powder, have been reported for these moieties (Van Dijk-Wolthuis et al 1997b). The very low intensity and broad shape of the Raman signal from the carbonate esters around 1750 cm^{-1} implies that intraphagosomal degradation of cross-linked dex-HEMA microspheres, which at pH values of 5–8 in the phagosome is likely to proceed predominantly by hydrolysis of these esters (Van Dijk-Wolthuis et al
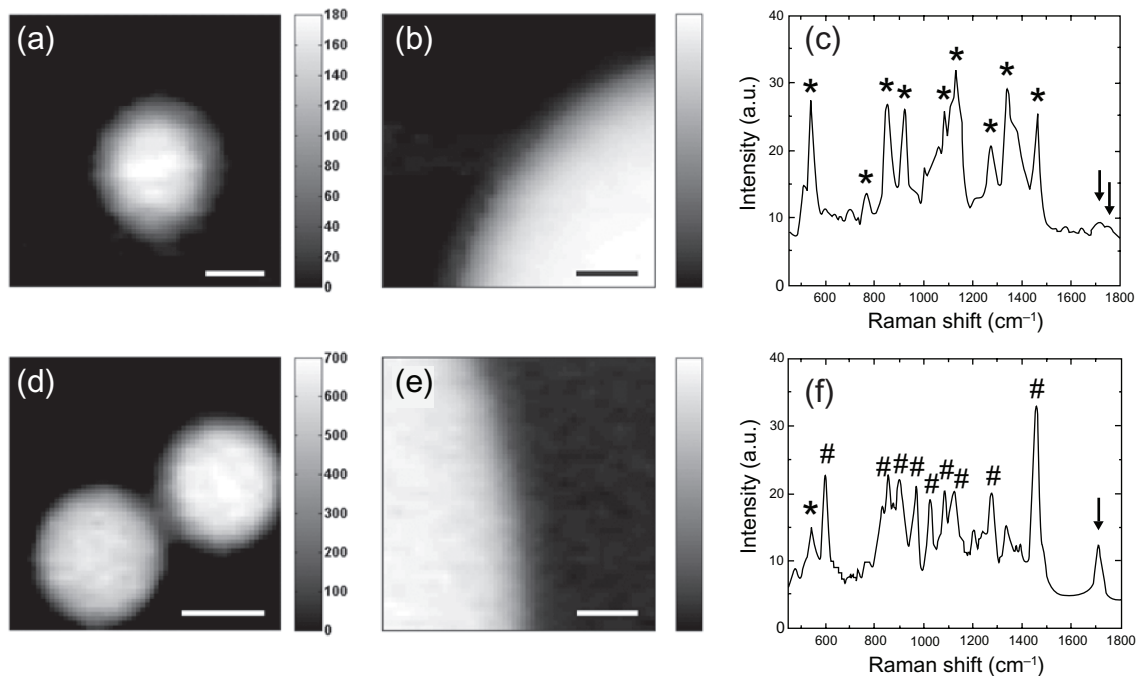

Figure 2 (**a**) and (**b**) Confocal Raman images, constructed from the intensity of the 541 cm^{-1} band of dextran, of freshly prepared dextran hydrogel microspheres (DS16). (**c**) Average Raman spectrum of the microsphere shown in (**a**). Strong signals assigned to dextran (Zhbankov et al 2000) are marked with asterisks. The overlapping broad bands centered at 1712 cm^{-1} and 1750 cm^{-1}, marked with arrows, probably originate from the methacrylate and carbonate ester bonds in dex-HEMA, respectively. (**d**) and (**e**) Confocal Raman images, constructed from the 1458-cm^{-1} band of poly(HEMA), of chemically hydrolyzed dextran hydrogel microspheres (DS16). (**f**) Average Raman spectrum, after buffer subtraction, of the microspheres shown in (**d**). Strong signals assigned to poly(HEMA) (Freddi et al 1996) are marked with crosses. Note the presence of residual dextran (asterisk) and the methacrylate ester C=O stretch vibration at 1711 cm^{-1} (arrow). Scale bars in (**a**) and (**d**) and in (**b**) and (**e**) represent 3.0 and 1.5 µm, respectively.

1997a), will be difficult to quantify by probing changes in this weak signal. Alternatively, a decrease in dextran concentration inside the microspheres, compared with fresh microspheres, may be taken as a sign of degradation, because carbonate ester hydrolysis and thus cross-link chain scission will result in free dextran chains that can subsequently diffuse out of the microspheres. We have followed the latter approach in quantifying intracellular microsphere degradation (*vide infra*).

To investigate the polymer distribution in chemically hydrolyzed dextran hydrogel microspheres by Raman microscopy, freshly prepared microspheres were heated overnight at 37 °C in 0.05 M NaOH. After several washing steps to remove dextran, Raman images of the resulting microspheres were recorded in the same way as decribed for the freshly prepared microspheres (*vide supra*). Representative images, constructed from the strong 1458 cm⁻¹ vibrational band, of hydrolyzed microspheres are shown in Figure 2d and 2e, and the average Raman spectrum of a hydrolyzed microsphere is shown in Figure 2f. From this spectrum the polymer after *in vitro* hydrolysis is unambiguously identified as poly(HEMA) (Freddi et al 1996). The presence of an intense band at 1711 cm⁻¹ (arrow in Figure 2f) indicates that the methacrylate ester bonds remain intact under the applied hydrolysis conditions, whereas the lack of a signal at 1750 cm⁻¹ suggests that all carbonate esters have been hydrolyzed. There is some residual dextran, as indicated by the Raman band at 541 cm⁻¹ (asterisk in Figure 2f).

It is clear from the Raman images in Figure 2 that the distribution of polymeric material is homogeneous, at least at the 0.33 μm spatial resolution of our setup, in both cross-linked dex-HEMA microspheres and in poly(HEMA) microspheres obtained after hydrolysis of dex-HEMA microspheres. This structural and chemically specific information, which can be obtained from intact microspheres without using labeling procedures, demonstrates the suitability of Raman microspectroscopy as a noninvasive technique for the investigation of biodegradable polymeric devices.

Raman microscopy of phagocytosed dextran hydrogel microspheres

We have previously used Raman microscopy to study PLGA microsphere degradation inside murine RAW 264.7 macrophages (Van Apeldoorn et al 2004). In the present study, we adhered cells of the same cell line to poly-L-lysine-coated CaF₂ slides and allowed them to phagocytose serum-opsonized cross-linked dex-HEMA microspheres (DS8 or DS16) for 3 h, followed by wash-

ing and continued incubation of the cells at 37 °C in culture medium for 1 week (DS8 microspheres) or 3 weeks (DS16 microspheres). After fixation of the cells using 2% paraformaldehyde, samples were investigated by Raman microscopy. In the case of DS8 microspheres, we also prepared a fixed sample directly after 3 h of phagocytosis in order to investigate intracellular microsphere degradation after 3 h.

Serum-opsonized dextran microspheres were efficiently phagocytosed by RAW 264.7 macrophages, as exemplified by the confocal Raman images shown in Figure 3.

Since polysaccharides typically make up ~6% of the dry mass of a mammalian cell (Alberts et al 2002) and therefore hardly contribute to cellular Raman spectra, the high concentration of dextran in cross-linked dex-HEMA microspheres allows the visualization of these microspheres inside macrophages by constructing Raman images from the strong vibrational band at 541 cm⁻¹ of dextran (Figure 3a). The Raman image constructed from the 1003 cm⁻¹ band of phenylalanine (Figure 3b) shows the expected homogeneous distribution of proteins throughout the cell. We also performed hierarchical cluster analysis (HCA) on Raman imaging data sets to visualize regions in cells with high Raman spectral similarities (Van Manen et al 2005). Average Raman spectra corresponding to different clusters can be used to assign clusters to particular cellular regions. For example, the average Raman spectra, shown in Figure 3d, of clusters 4 and 5 in Figure 3c indicate that these regions correspond to the dextran microsphere and the cell nucleus, respectively. The difference spectrum displayed in Figure 3e was obtained by subtracting the average Raman spectrum of cluster 3 from that of cluster 6. The presence of strong positive bands at 1003, 1300, 1440, and 1659 cm⁻¹ in this difference spectrum indicates that cluster 6 contains more proteins and lipids than cluster 3. We therefore assign cluster 6 to the endoplasmic reticulum and cluster 3 to the cytoplasm.

Raman microscopy experiments on microsphere-containing macrophages that had been cultured for 1–3 weeks in cell culture medium at 37 °C did not show morphological changes in the dextran microspheres (data not shown), which is in contrast to our previous results with PLGA microspheres (Van Apeldoorn et al 2004). However, polymer degradation may not necessarily lead to a loss of microsphere integrity, as demonstrated by the intact poly(HEMA) microspheres that remain after chemical hydrolysis of cross-linked dex-HEMA microspheres (*vide supra*). To establish whether degrada-
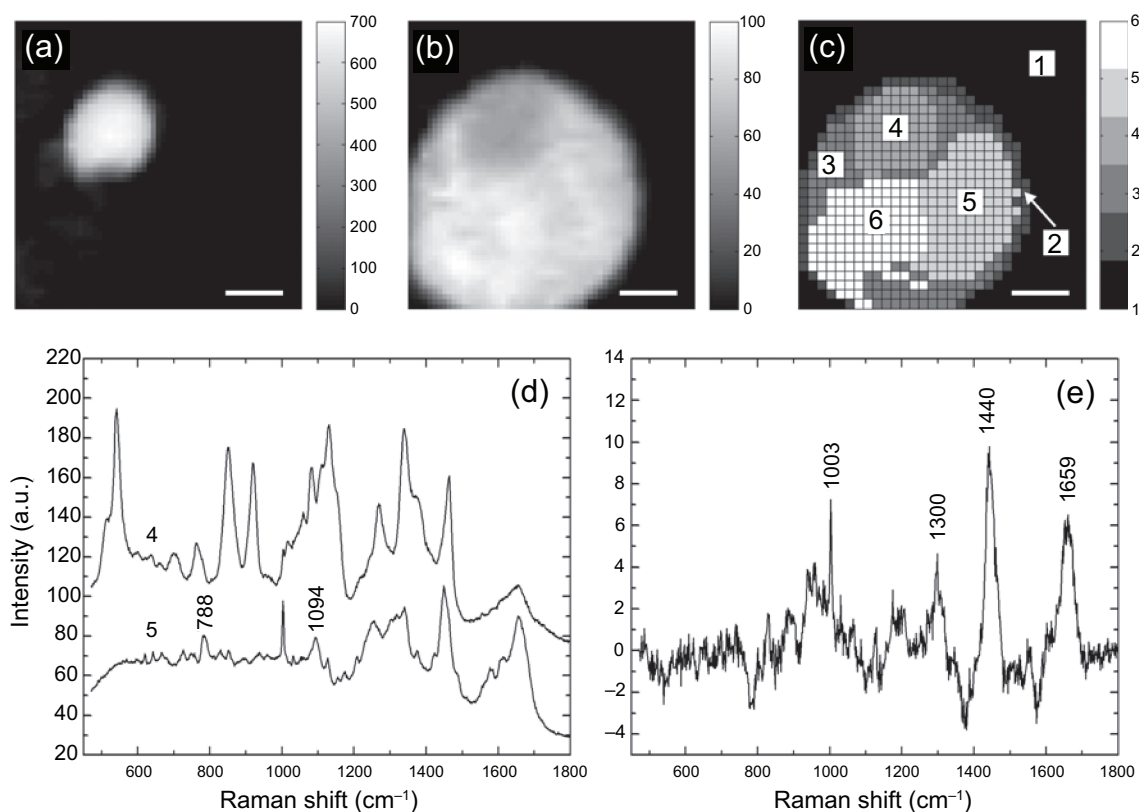
Figure 3 (**a**) and (**b**) Confocal Raman images, constructed from the intensity of the 541 cm⁻¹ band of dextran (**a**) and the 1003-cm⁻¹ band of phenylalanine (**b**), of a dextran hydrogel microsphere (DS8) internalized by a macrophage for 3 h. (**c**) Corresponding Raman hierarchical cluster analysis image. From their respective average Raman spectrum, clusters in this image are assigned to extracellular space (**1**), cell border (**2**), cytoplasm (**3**), microsphere (**4**), nucleus (**5**), and endoplasmic reticulum (**6**). (**d**) Average Raman spectra corresponding to clusters 4 and 5 in image (**c**). The bands at 788 and 1094 cm⁻¹ in spectrum 5, which arise from vibrational modes in the backbone of polynucleotides, indicate that cluster 5 in image (**c**) corresponds to the cell nucleus. Spectrum 4 has been shifted along the ordinate for clarity. (**e**) Raman difference spectrum obtained by subtracting the average spectrum of cluster 3 from the average spectrum of cluster 6 in image (**c**). From the positive bands at 1003, 1300, 1440, and 1659 cm⁻¹, originating from proteins and lipids, we assign cluster 6 in image (**c**) to endoplasmic reticulum (**ER**). Scale bars in (**a**), (**b**), and (**c**) represent 3.0 μm.

tion of dex-HEMA microspheres occurs in the phagosome of macrophages, we quantified the concentration of dextran inside phagocytosed microspheres by Raman spectroscopy, as described in the next section.

Quantification of the relative dextran concentration inside phagocytosed dextran hydrogel microspheres

We reasoned that a possible decrease of the weak and broad carbonate ester vibrational band at 1750 cm⁻¹ (see Figure 2c), which would signify intracellular microsphere degradation, would be difficult to quantify from Raman imaging data of macrophages with internalized cross-linked dex-HEMA microspheres. Therefore, we developed an alternative method that is based on quantification of the relative dextran concentration in phagocytosed microspheres, compared with freshly prepared microspheres, by Raman spectroscopy. A decrease in dextran concentration in degrading microspheres

is caused by swelling of the dex-HEMA microspheres and/or by dextran diffusion out of the microspheres. Previous in vitro experiments have shown that both macroscopic dex-HEMA hydrogels and dex-HEMA microspheres display an initial swelling phase followed by a dissolution phase, in which all dextran is liberated from the poly(HEMA) matrix and is released into the incubation medium (Franssen et al 1999). There is a delay time associated with the release of dextran, since the carbonate esters of all side chains linked to a single dextran chain must be hydrolyzed before release can occur. Both the swelling ratio and the dextran release delay time are strongly dependent on the degree of substitution of dex-HEMA.

We estimated the relative dextran concentration in the center of ingested microspheres by using the Raman band of water at 1640 cm⁻¹ as an internal intensity standard. By dividing the intensity of a vibrational band of dextran (eg, the strong 541-cm⁻¹ band) by the intensity of the 1640-cm⁻¹ water band (measured from Raman spectra taken outside

the cell), a ratio I_{dex}/I_{water} is obtained that is independent of day-to-day, sample-to-sample, and/or image-to-image variations in Raman detection efficiency, laser excitation power, focus heights above the substrate, etc. This procedure does not require additional measurements because spectra outside the cell are usually included in Raman mapping experiments of cells. Since the water concentration outside the cell is constant, changes in the I_{dex}/I_{water} ratio will reflect changes in the dextran concentration inside the microspheres. For a detailed description of our internal calibration procedure, see the Materials and methods section.

As shown in Figure 4, the I_{dex}/I_{water} ratio in DS8 dex-HEMA microspheres decreased from 3.61 (100%) in freshly prepared microspheres to 2.41 (67%) in phagocytosed microspheres that had been incubated for only 3 h with RAW 264.7 macrophages.

After 1 week of incubation time, the I_{dex}/I_{water} ratio in microspheres inside macrophages had further decreased to 2.03 (56%). For DS16 microspheres, the I_{dex}/I_{water} ratio decreased from 3.67 (100%) in freshly prepared microspheres to 1.85 (50%) in phagocytosed microspheres that had been incubated for 3 weeks with macrophages (Figure 4). The I_{dex}/I_{water} ratios found for undegraded DS8 (I_{dex}/I_{water} = 3.61) and DS16 (I_{dex}/I_{water} = 3.67) microspheres indicate that the dextran concentration inside these different microsphere types is similar. This may be expected, because the starting materials (dex-HEMA) used for the synthesis of DS8 and DS16 microspheres differ only in the number of HEMA side chains per dextran chain.
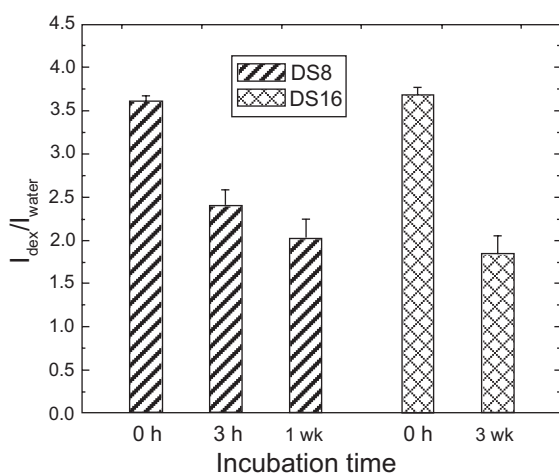

Figure 4 The relative concentration of dextran, I_{dex}/I_{water}, inside phagocytosed cross-linked dex-HEMA microspheres (DS8 and DS16) decreases in time upon incubation of microspheres with macrophages for the indicated times. The plotted I_{dex}/I_{water} ratios are mean + SD values of 2 (DS8, 0 h), 3 (DS8, 3 h), 5 (DS8, 1 wk), 2 (DS16, 0 h), and 8 (DS16, 3 wk) different dex-HEMA microspheres imaged by Raman microscopy.

In view of earlier work showing that swelling of dex-HEMA hydrogels precedes dextran release (Franssen et al 1999), the observed 33% initial decrease in dextran concentration in DS8 microspheres after 3 h of phagocytosis is probably caused by swelling of the microspheres. Occasionally, a very weak dextran Raman signal could be observed in cytoplasmic regions of the cell after 3 h of incubation (data not shown), suggesting that dextran has also been released from microspheres and diffused out of the phagosome to a minor extent at this time point. The large size of the dextran used (average molecular weight ~40 kDa) may hamper dextran diffusion across the phagosomal membrane, so the very weak Raman signal of dextran outside the phagosome does not necessarily rule out dextran release from microspheres. After 1 week of DS8 microsphere incubation with macrophages, we did not find an increased Raman signal of dextran in cytoplasmic regions of the macrophages, as compared with 3 h of incubation. This suggests that the further decrease in dextran concentration inside microspheres in this sample is again due to swelling. In DS16 microsphere-containing macrophages that had been incubated for 3 weeks (Figure 5a and 5b), we also observed a weak dextran Raman band at 541 cm^{-1} in regions outside of the microsphere, as exemplified by the point spectrum shown in Figure 5c taken from the asterisk-indicated cytoplasmic position in Figure 5a and 5b.

Together, the Raman microscopy results on DS8 and DS16 dextran microspheres phagocytosed by RAW 264.7 macrophages indicate a progressive degradation of these microspheres by swelling and, to a minor extent, dextran release. It will be of interest to investigate whether intracellular degradation within the time frames used here will already lead to the release of proteins that have been encapsulated by the microspheres. To that end, dextran microspheres may be loaded with a large tracer molecule such as green fluorescent protein (GFP) that is initially confined within the nanosized pores (Stenekes et al 2000) of the cross-linked dextran matrix. Release of the tracer from the microsphere into the cytoplasm upon degradation could then be studied by fluorescence microscopy. A similar approach has been reported for Texas red-labeled dextran (3 kDa) released from PLGA microspheres into the cytoplasm of mouse peritoneal macrophages (Newman et al 2000). Our initial studies indicate that GFP can be effectively encapsulated by cross-linked dex-HEMA microspheres and is distributed homogeneously throughout the microspheres (unpublished results), as was the case for FITC-labeled bovine serum albumin in a recently reported modeling study of protein release from cross-linked dex-HEMA microspheres (Vlugt-Wensink et al 2006).
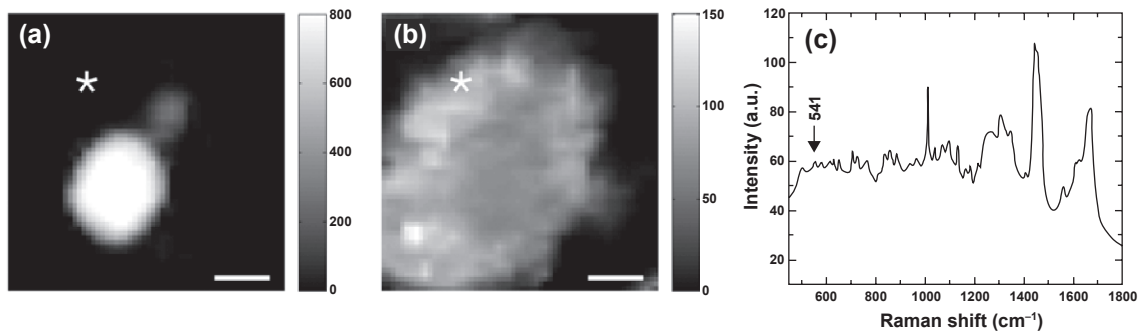
Figure 5 (**a**) and (**b**) Confocal Raman images, constructed from the intensity of the 541-cm⁻¹ band of dextran (**a**) and the 1003-cm⁻¹ band of phenylalanine (**b**), of a dextran hydrogel microsphere (DS16) internalized by a macrophage for 3 weeks. (**c**) Raman point spectrum of the cytoplasmic position marked with an asterisk in image (**a**) and (**b**). Note the presence of the weak dextran Raman band at 541 cm⁻¹, indicating that some dextran has diffused out of the microsphere. Scale bars in (**a**) and (**b**) represent 3.0 μm.

Raman microscopy of phagocytosed PEGT/PBT microspheres

Similar to cross-linked dextran microspheres, the biodegradation and drug release characteristics of microspheres composed of PEGT/PBT block copolymers have also been thoroughly studied, both in vitro and in vivo (Bezemer et al 2000c; Van Dijkhuizen-Radersma et al 2002, 2004a). However, the intracellular degradation of PEGT/PBT microspheres inside phagocytes has not been investigated. We therefore performed Raman microscopy experiments on RAW 264.7 macrophages that had been incubated with serum-opsonized PEGT/PBT microspheres for 1 week. We used hydrophilic 1000PEGT70PBT30 microspheres, in which the PEG molecular weight is 1000, the wt% of PEG terephthalate is 70, and the wt% of PBT is 30, because the high concentration of PEG in these microspheres results in faster degradation (Van Dijkhuizen-Radersma et al 2002) and protein release (Bezemer et al 2000c) than more hydrophobic PEGT/PBT microspheres with a lower PEG molecular weight and a higher wt% of PBT.

Similar to cross-linked dex-HEMA microspheres (*vide supra*), opsonized PEGT/PBT microspheres were efficiently phagocytosed by macrophages (Figure 6).

After 1 week of incubation, microspheres inside cells displayed the same morphology in optical microscopy images as microspheres that had not been phagocytosed (data not shown). By comparing scaled Raman point spectra taken from the center of microspheres inside and outside macrophages, we found no changes in Raman band intensities or spectral shifts upon phagocytosis for 1 week (Figure 7).

Furthermore, using Raman microscopy, we could not detect Raman bands of PEGT/PBT degradation products in the cytoplasm of microsphere-containing cells. Together, these results indicate that PEGT/PBT microspheres show little if any intracellular degradation within 1 week of

internalization by macrophages. This is in agreement with the very slow degradation reported for PEGT/PBT microspheres injected subcutaneously into rabbits (Van Dijkhuizen-Radersma et al 2002). In vitro degradation experiments (in PBS at 37 °C) of 1000PEGT71PBT29 microspheres revealed a gradual decrease in weight average molecular weight from 92.7 to 37.4 kg/mol in 24 weeks (Van Dijkhuizen-Radersma et al 2002). Perhaps longer incubation times in cell culture systems or measurements on microspheres retrieved from injection sites may lead to detectable changes in the Raman spectra of PEGT/PBT that are indicative of degradation. Indeed, by comparing Raman spectra of melt-pressed 1000PEGT70PBT30 discs before and after implantation for 12 weeks in rats, we have observed small but detectable changes in PEGT/PBT Raman band intensities that can be assigned to loss of PEGT from implanted discs (Van Apeldoorn 2005). Regarding cell culture experiments, we experienced problems with maintaining microsphere-containing cells (both dex-HEMA and PEGT/PBT microspheres) in a viable state beyond several weeks. Long incubation times typically led to cell detachment from
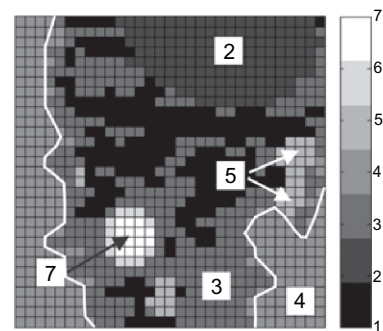

Figure 6 Hierarchical cluster image (8.9 × 8.9 μm²) of a PEGT/PBT microsphere internalized by a macrophage for 1 week. From their respective average Raman spectrum, clusters in this image are assigned to cell nucleus (**2**), cytoplasm (**3**), extracellular space (**4**), lipid droplets (**5**), and microsphere (**7**). The cell border is outlined in white.
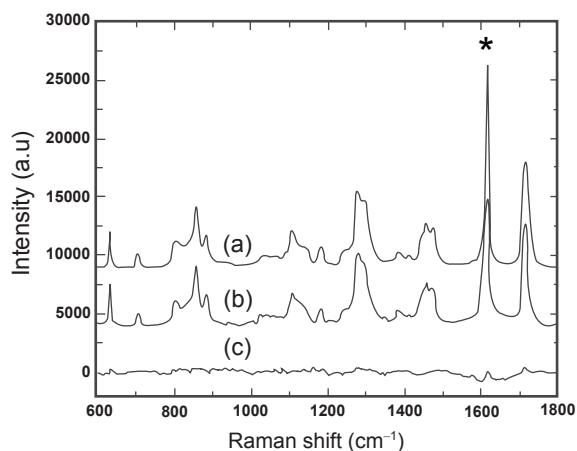
Figure 7 Confocal Raman point spectra taken from the center of PEGT/PBT microspheres located outside (**a**) and inside (**b**) macrophages. Cells were incubated with microspheres for 1 week. Spectra in (**a**) and (**b**), which were background-subtracted and scaled on the 1614-cm^{-1} band (marked with an asterisk), have been shifted along the ordinate for clarity. Difference spectrum (**c**) (spectrum (**a**) minus spectrum (**b**)) shows no changes in PEGT/PBT Raman band intensities or spectral shifts.

the substrate, resulting in cells being washed away during work-up. Presumably, the inflammatory and phagocytic response induced by internalization of microspheres (see also next section) causes cell necrosis or apoptosis. It is recommended that for intracellular degradation studies of PEGT/PBT microspheres in macrophages, more hydrophilic and faster degrading PEGT/PBT or related poly(ether-ester) copolymers (eg, butylene succinate-modified PEGT/PBT [Van Dijkhuizen-Radersma et al 2004b]) are taken.

Raman microscopy of macrophage foam cell formation induced by phagocytosis of microspheres

An important aspect in the application of biodegradable microspheres for drug delivery purposes is their biocompatibility. The subcutaneous implantation or injection of biodegradable macroscopic devices or microspheres, respectively, often leads to a tissue response by the host, which is characterized by the infiltration of specific cell types including neutrophils, macrophages, lymphocytes, and fibroblasts. Besides an inflammatory response caused by the accumulation of different leukocyte types at the implantation/injection site, contact of microspheres smaller than ~10 μm with phagocytes such as neutrophils and macrophages may lead to an additional phagocytic response, in which the microparticles are internalized and exposed to a degrading environment in the phagolysosome. The phagocytic process, which is a critical element of the innate immune response against invading microorganisms, has profound effects on the host immune cells. For example, to destroy ingested particles neutrophils produce large amounts of reactive oxygen species (ROS). Macrophages, while also able to produce ROS upon phagocytosis, secrete chemokines and cytokines to attract and activate other immune cells. Thus, injection of small microspheres may produce a more extensive tissue response than the injection of large microspheres or macroscopic implants that cannot be phagocytosed. Phagocytosis of microspheres also affects their biodegradation rate, as we recently demonstrated for PLGA microspheres in in vitro cell culture experiments (Van Apeldoorn et al 2004).

Whereas the tissue response to injected biodegradable microspheres is generally studied by histological techniques, much less is known about how microsphere phagocytosis affects the host cells. We therefore investigated the effect of microsphere internalization on macrophages at the single-cell level by Raman microscopy. Similar to recently reported results for PEGT/PBT microspheres (Van Manen et al 2006), we found that prolonged (≥1 week) incubation of dextran hydrogel microspheres with RAW 264.7 macrophages in cell culture led to the conversion of many macrophages into so-called "foam cells". Foam cells are the hallmark of early
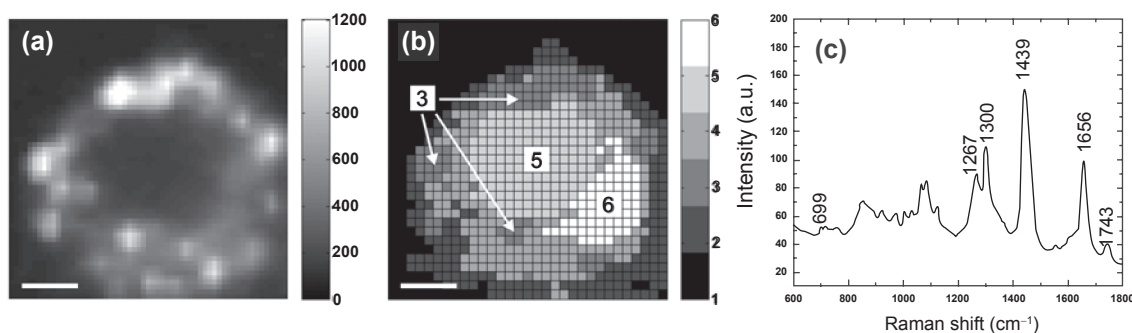

Figure 8 (**a**) Confocal Raman image, constructed from the 1656-cm^{-1} band of unsaturated lipids, of a RAW 264.7 macrophage that has been incubated with a DS8 dexHEMA microsphere for 1 week. (**b**) Corresponding hierarchical cluster analysis image. Clusters 3, 5, and 6 are assigned to lipid droplets, the dextran microsphere, and the cell nucleus, respectively. (**c**) Average Raman spectrum of cluster 3 in image (**b**). Scale bars in (**a**) and (**b**) represent 3.0 μm.

atherosclerotic lesions and are characterized by their high content of lipids (especially triglycerides and cholesterol esters) stored in intracellular lipid droplets (Li and Glass 2004; Rader and Puré 2005). The confocal Raman image displayed in Figure 8a, constructed from the 1656-cm^{-1} Raman band of unsaturated lipids, clearly shows the presence of many lipid droplets in a macrophage that has been incubated with a dex-HEMA microsphere for 1 week.

Figure 8b shows a hierarchical cluster image constructed from the same Raman imaging data set. Clusters 3, 5, and 6 in this image correspond to lipid droplets (three of which are marked with arrows), the dextran microsphere, and the cell nucleus, respectively. The strong Raman bands at 1267, 1300, 1439, and 1656 cm^{-1} in the average Raman spectrum of cluster 3 (Figure 8c) suggest that the lipid droplets are rich in unsaturated lipids. The weak band at 699 cm^{-1} indicates the presence of cholesterol or cholesterol esters in the lipid droplets, which confirms our reported results with PEGT/PBT microspheres (Van Manen et al 2006) and supports the large body of work identifying foam cells as cholesterol-laden cells (reviewed in Li and Glass 2004 and Rader and Puré 2005).

Conclusions

This study shows that confocal Raman microscopy is a versatile optical imaging technique to monitor intracellular degradation of polymeric microspheres in a quantitative, noninvasive and label-free manner. Raman imaging experiments on cross-linked dextran hydrogel microspheres and amphiphilic PEGT/PBT microspheres phagocytosed by macrophages for up to 3 weeks revealed that, whereas 1000PEGT70PBT30 microspheres do not show changes in their Raman spectra upon internalization by cells for 1 week, cross-linked DS8 and DS16 microspheres degrade in the phagolysosome by swelling, as evidenced by a decrease in the intensity of dextran vibrational bands in Raman spectra from phagocytosed microspheres. Moreover, phagocytosis of both types of microspheres induced the formation of macrophage foam cells, which were characterized by Raman microscopy as having intracellular lipid droplets rich in triglycerides and cholesterol (esters). Foam cell formation is likely an inflammatory response against the internalized polymeric microspheres, and may resemble the tissue response that occurs when microspheres or macroscopic devices are introduced into the body by subcutaneous injection or implantation.

We envisage that the scope of Raman microscopy can be extended beyond the level of imaging the degradation of microspheres in individual cells. The application of Raman microscopy on tissue sections may provide new histological information about injected or implanted biomaterials. Both drug delivery and tissue engineering applications could benefit from such an approach.

References

Alberts B, Johnson A, Lewis J, et al. 2002. Molecular Biology of the Cell. New York: Garland Science.

Allen TM, Cullis PR. 2004. Drug delivery systems: entering the mainstream. *Science*, 303:1818–22.

Anderson JM, Shive MS. 1997. Biodegradation and biocompatibility of PLA and PLGA microspheres. *Adv Drug Del Rev*, 28:5–24.

Banchereau J, Steinman RM. 1998. Dendritic cells and the control of immunity. *Nature*, 392:245–52.

Bezemer JM, Grijpma DW, Dijkstra PJ, et al. 1999. A controlled release system for proteins based on poly(ether-ester) block-copolymers: polymer network characterization. *J Control Release*, 62:393–405.

Bezemer JM, Radersma R, Grijpma DW, et al. 2000a. Zero-order release of lysozyme from poly(ethylene glycol)/poly(butylene terephthalate) matrices. *J Control Release*, 64:179–92.

Bezemer JM, Radersma R, Grijpma DW, et al. 2000b. Microspheres for protein delivery prepared from amphiphilic multiblock copolymers 1. Influence of preparation techniques on particle characteristics and protein delivery. *J Control Release*, 67:233–48.

Bezemer JM, Radersma R, Grijpma DW, et al. 2000c. Microspheres for protein delivery prepared from amphiphilic multiblock copolymers 2. Modulation of release rate. *J Control Release*, 67:249–60.

Butcher EC, Berg EL, Kunkel EJ. 2004. Systems biology in drug discovery. *Nat Biotechnol*, 22:1253–1259.

Cadée JA, Brouwer LA, Den Otter W, et al. 2001. A comparative biocompatibility study of microspheres based on cross-linked dextran or poly(lactic-co-glycolic)acid after subcutaneous injection in rats. *J Biomed Mater Res*, 56:600–9.

Chan JW, Taylor DS, Zwerdling T, et al. 2006. Micro-Raman spectroscopy detects individual neoplastic and normal hematopoietic cells. *Biophys J*, 90:648–56.

Cleland JL, Daugherty A, Mrsny R. 2001. Emerging protein delivery methods. *Curr Opin Biotechnol*, 12:212–19.

Crommelin DJA, Storm G, Verrijk R, et al. 2003a. Shifting paradigms: biopharmaceuticals versus low molecular weight drugs. *Int J Pharm*, 266:3–16.

Crommelin DJA, Storm G, Jiskoot W, et al. 2003b. Nanotechnological approaches for the delivery of macromolecules. *J Control Release*, 87:81–8.

De Groot CJ, Cadée JA, Koten J-W, et al. 2002. Therapeutic efficacy of IL-2-loaded hydrogels in a mouse tumor model. *Int J Cancer*, 98:134–40.

Deschamps AA, Van Apeldoorn AA, Hayen H, et al. 2004. In vivo and in vitro degradation of poly(ether ester) block copolymers based on poly(ethylene glycol) and poly(butylene terephthalate). *Biomaterials*, 25:247–58.

Edlund U, Albertsson A-C. 2002. Degradable polymer microspheres for controlled drug delivery. *Adv Polym Sci*, 157:67–112.

Feldmann M, Steinman L. 2005. Design of effective immunotherapy for human autoimmunity. *Nature*, 435:612–9.

Franssen O, Vandervennet L, Roders P, et al. 1999. Degradable dextran hydrogels: controlled release of a model protein from cylinders and microspheres. *J Control Release*, 60:211–2.

Freddi G, Massafra MR, Beretta S, et al. 1996. Structure and properties of *Bombyx mori* silk fibers grafted with methacrylamide (MAA) and 2-hydroxyethyl methacrylate (HEMA). *J Appl Polym Sci*, 60:1867–76.

Greenberg S, Grinstein S. 2002. Phagocytosis and innate immunity. *Curr Opin Immunol*, 14:136–45.

Gupta P, Vermani K, Garg S. 2002. Hydrogels: from controlled release to pH-responsive drug delivery. *Drug Discov Today*, 7:569–79.

Hoffman AS. 2002. Hydrogels for biomedical applications. *Adv Drug Deliv Rev*, 43:3–12.

Joyce AR, Palsson BØ. 2006. The model organism as a system: integrating "omics" data sets. *Nat Rev Mol Cell Biol*, 7:198–210.

Krafft C, Knetschke T, Funk RHW, et al. 2006. Studies on stress-induced changes at the subcellular level by Raman microspectroscopic mapping. *Anal Chem*, 78:4424–29.

Kumar N, Ravikumar MNV, Domb AJ. 2001. Biodegradable block copolymers. *Adv Drug Deliv Rev*, 53:23–44.

Li AC, Glass CK. 2004. The macrophage foam cell as a target for therapeutic intervention. *Nat Med*, 8:1235–42.

Newman KD, Kwon GS, Miller GG, et al. 2000. Cytoplasmic delivery of a macromolecular fluorescent probe by poly(d,l-lactic-co-glycolic acid) microspheres. *J Biomed Mater Res*, 50:591–7.

Nikolsky Y, Nikolskaya T, Bugrim A. 2005. Biological networks and analysis of experimental data in drug discovery. *Drug Discov Today*, 10:653–62.

Notingher I, Hench LL. 2006. Raman microspectroscopy: a noninvasive tool for studies of individual living cells in vitro. *Expert Rev Med Devices*, 3:215–34.

Panyam J, Labhasetwar V. 2003. Biodegradable nanoparticles for drug and gene delivery to cells and tissue. *Adv Drug Deliv Rev*, 55:329–47.

Peppas NA, Bures P, Leobandung W, et al. 2000. Hydrogels in pharmaceutical formulations. *Eur J Pharm Biopharm*, 50:27–46.

Rader DJ, Puré E. 2005. Lipoproteins, macrophage function, and atherosclerosis: Beyond the foam cell? *Cell Metab*, 1:223–30.

Raychaudhuri S, Rock KL. 1998. Fully mobilizing host defense: Building better vaccines. *Nat Biotechnol*, 16:1025–31.

Schellekens H. 2002. Bioequivalence and the immunogenicity of biopharmaceuticals. *Nat Rev Drug Discov*, 1:457–62.

Sinha VR, Trehan A. 2003. Biodegradable microspheres for protein delivery. *J Control Release*, 90:261–80.

Stenekes RJH, Franssen O, Van Bommel EMG, et al. 1998. The preparation of dextran microspheres in an all-aqueous system: effect of the formulation parameters on particle characteristics. *Pharm Res*, 15:557–61.

Stenekes RJH, De Smedt SC, Demeester J, et al. 2000. Pore sizes in hydrated dextran microspheres. *Macromolecules*, 1:696–703.

Stenekes RJH, Loebis AE, Fernandes CM, et al. 2001. Degradable dextran microspheres for the controlled release of liposomes. *Int J Pharmaceut*, 214:17–20.

Stoughton RB, Friend SH. 2005. How molecular profiling could revolutionize drug discovery. *Nat Rev Drug Discov*, 4:345–50.

Uzunbajakava N, Lenferink A, Kraan Y, et al. 2003. Nonresonant confocal Raman imaging of DNA and protein distribution in apoptotic cells. *Biophys J*, 84:3968–81.

Van Apeldoorn AA, Van Manen H-J, Bezemer JM, et al. 2004. Raman imaging of PLGA microsphere degradation inside macrophages. *J Am Chem Soc*, 126:13226–7.

Van Apeldoorn AA. 2005. Confocal Raman Microscopy: Applications in tissue engineering. PhD thesis, University of Twente, The Netherlands.

Van de Weert M, Hennink WE, Jiskoot W. 2000. Protein instability in poly(lactic-co-glycolic acid) microparticles. *Pharm Res*, 17:1159–67.

Van Dijkhuizen-Radersma R, Hesseling SC, Kaim PE, et al. 2002. Biocompatibility and degradation of poly(ether-ester) microspheres: in vitro and in vivo evaluation. *Biomaterials*, 23:4719–29.

Van Dijkhuizen-Radersma R, Wright SJ, Taylor LM, et al. 2004a. In vitro/in vivo correlation for ^{14}C-methylated lysozyme release from poly(ether-ester) microspheres. *Pharm Res*, 21:484–91.

Van Dijkhuizen-Radersma R, Roosma JR, Sohier J, et al. 2004b. Biodegradable poly(ether-ester) multiblock copolymers for controlled release applications: An in vivo evaluation. *J Biomed Mater Res*, 71A:118–27.

Van Dijk-Wolthuis WNE, Van Steenbergen MJ, Underberg WJM, et al. 1997a. Degradation kinetics of methacrylated dextrans in aqueous solution. *J Pharm Sci*, 86:413–17.

Van Dijk-Wolthuis WNE, Tsang SKY, Kettenes-van den Bosch JJ, et al. 1997b. A new class of polymerizable dextrans with hydrolyzable groups: hydroxyethyl methacrylated dextran with and without oligo-lactate spacer. *Polymer*, 38:6235–42.

Van Manen H-J, Kraan YM, Roos D, et al. 2004. Intracellular chemical imaging of heme-containing enzymes involved in innate immunity using resonance Raman microscopy. *J Phys Chem B,* 108:18762–71.

Van Manen H-J, Kraan YM, Roos D, et al. 2005. Single-cell Raman and fluorescence microscopy reveal the association of lipid bodies with phagosomes in leukocytes. *Proc Natl Acad Sci U S A*, 102:10159–64.

Van Manen H-J, Van Apeldoorn AA, Roos D, et al. 2006. Raman microscopy of phagocytosis: shedding light on macrophage foam cell formation. In: Mahadevan-Jansen A, Petrich WH eds. Biomedical Vibrational Spectroscopy III: Advances in Research and Industry. Proc. of SPIE Vol. 6093, 60930I1–9.

Vlugt-Wensink KDF, Vlugt TJH, Jiskoot W, et al. 2006. Modeling the release of proteins from degrading cross-linked dextran microspheres using kinetic Monte Carlo simulations. *J Control Release*, 111:117–27.

Zhbankov RG, Firsov SP, Korolik EV, et al. 2000. Vibrational spectra and the structure of medical biopolymers. *J Mol Struct*, 555:85–96.